### Title
Developing a Control Strategy for Minimum Airflow Setting Considering CO2 Level and Energy Consumption in a Variable Air Volume System




### Journal
International Journal of Thermophysics, 45(12)

### ISSN
0195-928X



### Authors
Lee, Jong Man
Lee, Kwang Ho
Moon, Jin Woo
et al.



### Publication Date
2024-12-01

### DOI
10.1007/s10765-024-03474-5

International Journal of Thermophysics (2024) 45:173
https://doi.org/10.1007/s10765-024-03474-5

# Developing a Control Strategy for Minimum Airflow Setting Considering $CO_2$ Level and Energy Consumption in a Variable Air Volume System

**Jong Man Lee[1] · Kwang Ho Lee[1] · Jin Woo Moon[2] · Sang Hoon Lee[3] · Tianzhen Hong[3]**

Received: 27 September 2024 / Accepted: 15 November 2024 / Published online: 26 November 2024


## Abstract
In an office building equipped with a Variable Air Volume (VAV) system, this paper introduces a novel method for controlling the minimum supply airflow fraction in each zone's VAV box, having a capability to consider indoor $CO_2$ level and energy consumption. The EnergyPlus simulation using the medium office prototype model was employed, which evaluated the performance of the energy and $CO_2$ concentration for five VAV box airflow control strategies. The paper focuses on $CO_2$ concentration-based airflow control method and compares it with other four methods including conventional single-max, reduced minimum single-max, demand-controlled ventilation(DCV), and dualmax control methods according to guidelines and common practices. The newly proposed control strategy directly correlates the minimum airflow fraction to $CO_2$ concentration. A general trend emerged when comparing $CO_2$ concentrations—lower minimum airflow fractions were associated with higher concentrations. The proposed control method effectively maintained low $CO_2$ concentrations and enabled a lower airflow fraction contributing to energy consumption reduction. It was confirmed that heating energy consumption in climate zone 4A, 5B, and 6A showed a maximum saving of approximately 30% compared to the conventional single-max and dual max control strategies. It was found that cooling energy consumption in climate zone 4A and 6A can achieve a maximum saving of approximately 10% compared to the conventional control strategies. The proposed $CO_2$ concentration-based control logic is promising as it not only improves the indoor air quality lowering the $CO_2$ concentration in the occupied spaces, but also contributes to HVAC energy savings.

**Keywords** $CO_2$ concentration · HVAC energy consumption · Indoor air quality · Office building · Variable air volume system

Extended author information available on the last page of the article

## 1 Introduction

The indiscriminate use of fossil fuels is contributing to environmental degradation and global climate issues, including air pollution and greenhouse gas emissions [1]. Worldwide eff ts are underway to decarbonize, with sector-specifi measures and policies being deliberated at the Conference of Paris [2]. Among various sectors, building operations account for 30% of global $CO_2$ emissions [3]. As population growth and economic development persist, building fl areas are expected to expand, leading to a likely increase in emissions [4]. Therefore, it is imperative to implement measures at the individual building level to reduce energy consumption, which contributes to emission reduction [5]. This paper explores an approach to reduce energy consumption in heating, ventilation, and air-conditioning (HVAC) systems in buildings.

In conventional HVAC systems, elements directly associated with heating and cooling energy include the air handling unit (AHU), chiller, boiler, variable air volume (VAV), and constant air volume (CAV) systems [6]. Among these, the VAV system is widely used in various building types such as offi buildings and commercial structures. The VAV system adjusts airfl w and temperature as necessary to meet the setpoint temperature and to maintain occupants' thermal comfort [7].

In the realm of building energy management, the optimization of HVAC systems plays a pivotal role in achieving sustainability and effi . The following research provide a comprehensive overview that collectively contributes to advancing VAV box control strategies, specifi y focusing on minimizing energy consumption in commercial and offi buildings. The study by Jee et al. introduced a groundbreaking approach to HVAC control, utilizing machine learning for simultaneous control of AHU discharge air and condenser water temperatures [8]. Lee et al. explored the application of artifi neural networks in optimizing AHU discharge air temperature setpoints, specifi y targeting minimized cooling energy in VAV systems [9]. Building upon the foundation of energy modeling and model predictive control, Kim et al. presented a comprehensive review of current research trends in HVAC systems [10].

While much of the research on VAV systems has focused on control methods and strategies, with some emphasis on energy savings and performance, studies have also delved into ventilation and system elements such as supply air temperature and airfl w directly related to VAV systems.

Zhang et al. evaluated the savings potential of occupancy-based control of terminal boxes for large offi buildings with VAV HVAC systems using both common and advanced occupancy sensors [11]. Wang et al. explored the energy-saving potential of occupancy-based controls, analyzing the energy-saving capabilities of a control method using rule-based control algorithms applicable to existing offi buildings with VAV systems [12]. Niu et al. investigated a model-based optimal control strategy aimed at minimizing energy consumption in the heating mode of a building HVAC system [13]. Choi et al. compared energy consumption characteristics and indoor environment based on VAV system control methods, providing foundational data for energy-saving and comfortable indoor environments [14]. Ji et al. employed a decoupled control technique based on a wavelet neural network to eliminate coupling between temperature and humidity control loops in a VAV system [15]. Feng et al. experimentally studied the relationship between valve opening, static pressure, and air volume to control air volume [16]. Kim and Cho utilized artifi neural networks to optimize the supply airfl w rate and temperature of VAV terminal devices [17]. Li et al. proposed a real-time optimal control strategy adopting a multi-agent-based distributed optimization method for multizone VAV air-conditioning systems [18]. Li et al. aimed to control the time delay of indoor temperature in a VAV air-conditioning system, presenting an indoor temperature prediction control method based on the Elman neural network multistep prediction model [19]. Ma et al. proposed a coordination strategy for distributed model predictive control to coordinate AHU and VAV boxes in a multizone HVAC system [20]. Nasirpour and Balochian designed a multivariate unlocked fractional order PID (FOPID) (PIlDm) controller for VAV systems [21]. Rahnama et al. investigated the energy-saving potential of a novel mechanical ventilation system by replacing terminal dampers with decentralized fans [22, 23]. Seong et al. developed a real-time optimal control strategy for VAV air conditioning in HVAC systems using genetic algorithms and a simulated large-scale offi building [24]. Zhang et al. developed a model-based control method to achieve decoupling control of room temperature and humidity based on the bilinear characteristics of temperature and humidity variations in a VAV air-conditioning system [25]. Zhu et al. presented a coupled simulation of computational fl dynamics (CFD) and building energy simulation for a VAV system in an offi building located in Shanghai to simulate the building, VAV control system, and indoor thermal environment simultaneously [26].

Meng et al. developed a multizone VAV and variable water volume (VWV) air-conditioning system [27]. Meng et al. presented a system-level global optimization approach to minimize energy consumption in multizone VAV and VWV air-conditioning systems [28]. Pang et al. conducted a study to characterize the variations among VAV system controls and proposed a method to define the baseline VAV system performance for different use cases [29]. Saber investigated the impact of the minimum airflow fraction (MAFF) on various performance aspects of a multiple-zone variable air volume reheat (VAVR) design in different building applications and climate types [30]. Zhang et al. presented work on the development and verifica- tion of the ASHRAE Guideline 36–2018 control sequences for single-zone variable air volume AHU systems [31]. Zhang et al. evaluated the energy use of a multizone VAV system with terminal reheating using ASHRAE Guideline 36 sequences and compared it to a group of baseline control sequences that represent existing prac- tices [32].

Kapalo and Spodyniuk compared a ventilation system with a constant flow of ventilated air with an air-conditioning system with varying airflow rates to ensure the required air quality [33]. Alghamdi evaluated the various impacts of integrating multizone VAV systems with Dedicated Outdoor Air Systems (DOAS), focusing on energy consumption, thermal comfort, and lifecycle costs [34]. Kaam et al. developed and tested a time-averaged ventilation (TAV) control strategy in an institutional building on the UC Berkeley campus [35]. Kim and Cho proposed a control method with a ventilation requirement for the VAV terminal unit and AHU in multiple zones [36]. Lee et al. simulated the performance of a conventional VAV unit system applied to a typical office building prototype, evaluating the energy impact of the minimum airflow setting of a VAV box [37].

Previous studies have shown that occupancy-based control strategies, particularly those that adjust the minimum air flow rate of VAV boxes based on $CO_2$ concentration, can significantly improve energy efficiency. By monitoring the occupancy of each space using $CO_2$ sensors, the system can supply only the required ventilation, preventing excessive energy consumption. By monitoring and controlling $CO_2$ concentrations, the ventilation requirements of each space can be met more accurately. High $CO_2$ levels indicate that the space is poorly ventilated and has high occupancy. $CO_2$-based control strategies contribute to improving indoor air quality, ensuring a healthy and comfortable environment inside the building. Therefore, this study aims to introduce a straightforward and efficient control approach designed to enhance both ventilation and energy efficiency within a VAV system used in commercial buildings. Our goal is to develop a control method that can improve energy efficiency and maintain proper indoor air quality by controlling the minimum airflow fraction in relation to $CO_2$ concentration. As an initial step in our research, we aim to compare and contrast the changes in indoor air quality, with a specific focus on $CO_2$ concentration, and energy consumption when controlling the minimum airflow fraction based on $CO_2$ levels in occupied spaces. This comparison will be made against other control scenarios to elucidate the effectiveness of our proposed control method in maintaining optimal indoor air quality while enhancing energy efficiency.

## 2 Methods

### 2.1Simulation Model

Building energy simulations were conducted to implement the proposed control strategy and compare its performance against the existing methods. The simulation utilized version 9.3 of the EnergyPlus program, developed by the U.S. Department of Energy (DOE) [38]. EnergyPlus was chosen for its suitability in modeling an office building with a VAV system, and it incorporates the VAV system control method for each case [39]. Furthermore, EnergyPlus offers essential functions for implementing $CO_2$ concentration-based control in the simulation, which is the focus of this study. The Energy Management Simulation (EMS) function facilitates the implementation of control methods or algorithms that cannot be achieved through built-in features, using the EnergyPlus Runtime Language (ERL) [40]. To explain a little more about EMS, to use the EMS functionality in EnergyPlus for simulation, a Sensor, Program, and Actuator object must be set up. First, through the sensor object, a user must choose which value (e.g., temperature or humidity) to apply the EMS function to, and the selected value through Sensor object must be implemented into ERL through Program object. Furthermore, by specifying in Program object which Actuator object (e.g., chiller or fan) the implemented logic will be applied to, the user can utilize the basic functions of the EMS [41, 42].

A cold and humid climate condition of Rochester, Minnesota, USA was used to evaluate the VAV control methods, which corresponds to climate zone 6A on the International Energy Conservation Code (IECC) [43]. The medium office model used in the simulation is depicted in Fig. 1. The simulated building, a three-story medium office building, was specified differently from reference models in prior studies, such as the floor plan, the indoor spaces are represented in detail [44]. The new prototype model is specifically tailored to suit the needs of small to medium-sized office buildings, incorporating customized additional space types such as open office, enclosed office, conference room, restroom, and corridor. Furthermore, the number of occupants, internal heat gain conditions(electric equipment, lighting, and ventilation) for these new space types have been defined according to ASHRAE Standard 90.1 and 62.1 [44]. The model comprised 23 zones on the bottom floor, 21 zones on the middle and top floors, and 65 zones (excluding the plenum), as shown in the floor plan. The main occupancy spaces included open offices, closed offices (enclosed offices), and conference rooms (confidential). Other areas included a lobby, storage, corridor, dining, stairs, restroom, and mechanical room [44]. The target spaces for the analysis in this study are Open Office 1 and 2, Conference Room 1 and 2 and Enclosed Office 1 through 3. Those zones were chosen to see how the difference in infiltration and occupancy scheduling among zones would differently be affected by the proposed control logic.

Table 1 outlines the areas for office space and conference rooms corresponding to the main occupied zones in this model.

Figure 2 illustrates HVAC system configuration. HVAC system is described as follows: AHU installed on each floor contains a direct expansion (DX) coil (for

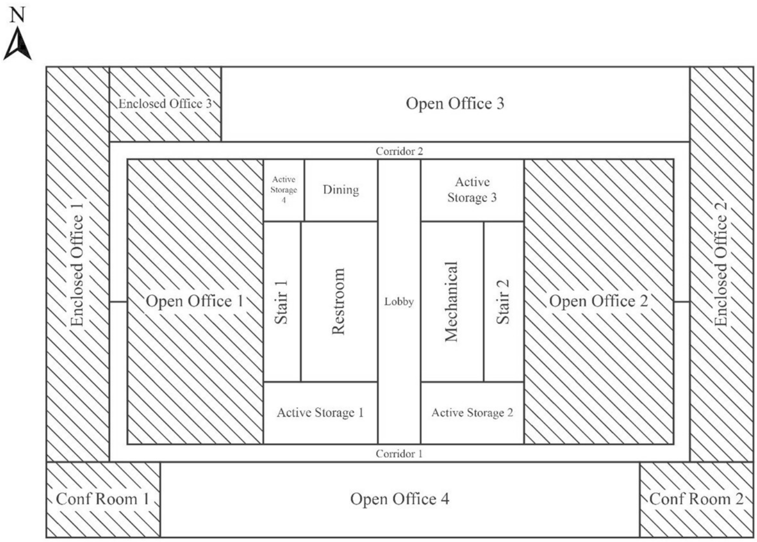


Fig. 1 Reference building floor plan [44]

**Table 1** Target zone information

| Type | Area [m$^2$] |
|---|---|
| Open Office Bottom/Middle/Top floor 1 zone | 194 |
| Open Office Bottom/Middle/Top floor 2 zone | 212 |
| Enclosed Office Bottom/Middle/Top floor 1 and 2 zone | 125 |
| Enclosed Office Bottom floor 3 and 4 zone | 45 |
| Enclosed Office Middle/Top floor 3 zone | 42 |
| Conf Room Bottom/Middle/Top floor 1 and 2 zone | 43 |

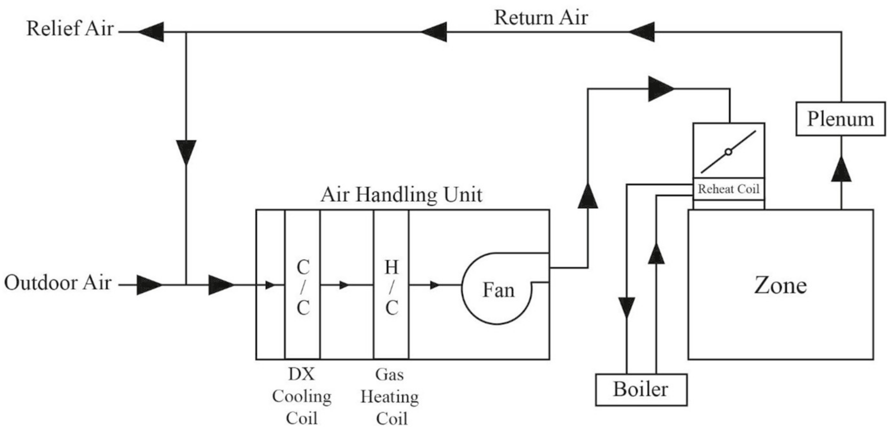


**Fig. 2** HVAC system configuration

cooling), a gas heating coil (for heating), and an AHU supply fan. The air delivered from the AHU passes through a VAV terminal unit applied to each zone (65 zones). The VAV terminal unit includes a reheat coil, which uses hot water from one boiler for reheating at the VAV terminal unit in the entire zone. The air from the zone that has passed through the VAV terminal unit is returned back into the plenum of each floor, mixed with the outdoor air through the economizer, and circulated again. The AHU supply fan and DX coil use electricity, while the gas heating coil and boiler use gas as an energy source.

The heating setpoint is configured at 21 °C on weekdays from 7:00 to 22:00, 21 °C on Saturdays from 7:00 to 18:00, and 21 °C for 24 h on winter design days. Cooling setpoints are maintained at 24 °C on weekdays from 7:00 to 22:00 and 24 °C on Saturdays from 7:00 to 18:00, aligning with the summer design day schedule.

## 2.2 Simulation Cases

The control methods proposed in this study, along with the other cases for comparison in simulations, are outlined in Table 2. Notably, the Single-Max (conventional

**Table 2** Simulation cases description

| | Conventional single-max (Fig. 3) | Reduced minimum single-max (VAV minimum retune) | DualMax (Fig. 4) | DCV (Demand-controlled ventilation) | CO2 Based (Fig. 6) |
|---|---|---|---|---|---|
| VAV minimum tion | 30% (Single maximum logic) | 15% (Single maximum logic) | 30% (Minimum) | 30% (Conditional) | 10% to 30% (conditional, Single |
| Control strategy | Fraction is always constant | Fraction is always constant | Adopt reverse with limit (dual maximum logic) in EnergyPlus | - Adapted indoor air quality procedure (IAQP) algorithm for DCV<br>- When $CO_2$ concentration over the setpoint, VAV minimum airflow fraction is set to 30% | Sets VAV minimum airflow fraction within the specified indoor $CO_2$ setpoint range |

single-max) and DualMax cases, applied to the VAV system by default, are set based on reference values. The reduced minimum single-max case reduces the minimum airflow fraction in the VAV system to 15%, and demand-controlled ventilation (DCV) adjusts ventilation based on $CO_2$ concentration, mirroring the proposed con- trol method. Additionally, a new $CO_2$-based control method is proposed, which has the capability to consider indoor $CO_2$ level and energy consumption.

Figure 3 illustrates the single-maximum control logic among the VAV control methods. This logic, representing the conventional single-max case (minimum airflow setpoint 30% in heating loop) and reduced minimum single-max case (minimum airflow setpoint 15% in heating loop) in this study, involves maximum airflow setpoint in the cooling loop. The $CO_2$-based control method proposed in this study follows a similar single-maximum control logic. The control options for the damper controlling airflow during the heating operation of single-maximum control logic are as follows: When the zone temperature is between the cooling and heating setpoints and within the dead band, the damper of the VAV terminal unit maintains the airflow rate at a minimum. As the heating load increases, the water flow rate of the reheat coil is increased to the maximum or until the reheat air temperature set by the user is reached [45].

Figure 4 is an illustration of the dual maximum control logic of the VAV control method. Unlike the single-maximum control logic, the heating loop is also characterized by the addition of a maximum heating airflow setpoint. This control logic corresponds to DualMax case in this study. Dual maximum control logic operates as follows: when the heating load increases, the unit starts operating with minimum airflow and minimum hot-water flow. As the hot-water flow increases until reaching the maximum flow or the maximum reheat air temperature determined by the user, the damper opens to handle the load. The damper can only partially open up to the specified maximum flow rate [45].

During the simulation, DCV adjusts the ventilation rate based on occupancy or indoor air quality (IAQ). This process, utilizing sensing or IAQ monitoring, reduces airflow in unoccupied spaces and increases airflow in occupied spaces, minimizing unnecessary energy wastage. This approach is particularly effective in building types

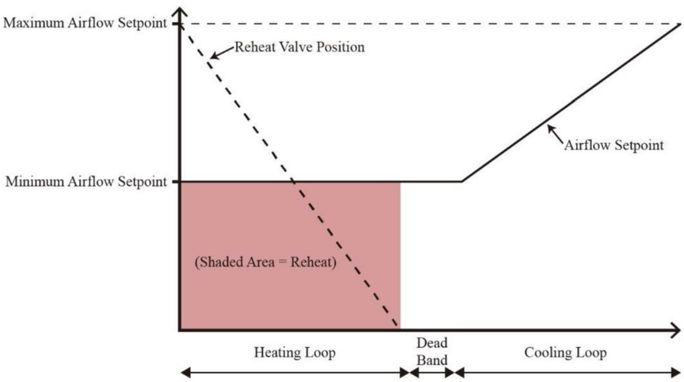

Fig. 3 Single-maximum control logic [45]

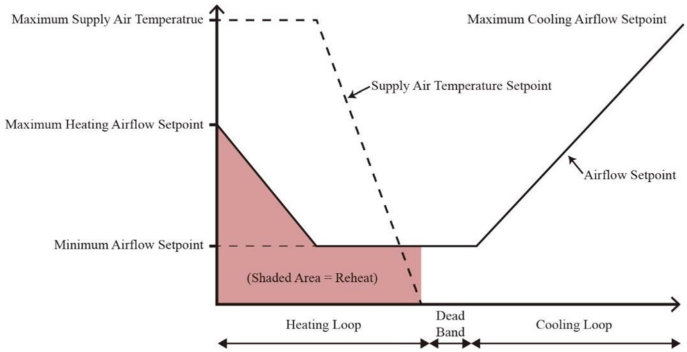


**Fig. 4** Dual maximum control logic [45]

with fluctuating occupancy, such as educational, office, and commercial buildings, offering energy savings while maintaining proper IAQ [46]. In the study, DCV was applied using the Indoor Air Quality Procedure (IAQP) to calculate the outdoor air flow required to meet the $CO_2$ setpoint specified by the user for each zone through the terminal units. The $CO_2$ setpoint is configured with minimum and maximum thresholds, where the minimum is set at 400 ppm and the maximum is adjusted according to the characteristics of each zone, consistent with Table 7 and Title 24. Additionally, DCV was applied to 35 out of the total 65 zones(except corridor, mechanical, restroom, stair, and active storage zones of each floor), and the outdoor airflow settings for the three-zone groups(Open Office zones, Enclosed Office zones, and Conference Room zones) relevant to the analysis target are all approximately 0.0094 $m^3 \cdot s^{-1}$*person [45].

The proposed VAV system control method simplifies the control mechanism compared to the DCV method, requiring fewer parameters and streamlining the control process. In addition, the $CO_2$ concentration-based control method directly correlates the minimum airflow fraction, crucial for ventilation, to $CO_2$ concentration, optimizing energy consumption in response to immediate occupancy changes. The proposed method regulates the minimum airflow of the VAV system installed in each zone based on the $CO_2$ concentration level, thereby conserving energy, particularly reheat energy, by delivering only the required amount of airflow to each zone. The maximum airflow rate is 30%, and the minimum airflow rate is 10%, which is set by the user. This allows the proposed control method to provide adequate ventilation without over-ventilating spaces with sudden changes in occupancy, resulting in high potential energy savings. Figure 5 describes the control logic proposed in the study.

In the $CO_2$-Based case, the VAV minimum airflow fraction is set to the lowest when indoor $CO_2$ concentration is at its lowest and the highest when it exceeds the recommended value according to ASHRAE Standard 62.1 or California Title 24. Between the maximum and minimum setpoints, $CO_2$ concentration linearly controls the minimum airflow fraction. This control logic utilizes the EMS functionality of the EnergyPlus program, implementing target zones to control the minimum airflow

*IF (Zone Air CO2 Concentration $\leq$ Indoor Low CO2 Concentration)*

$$VAV\ Minimum\ Airflow\ Fraction = Fraction\ at\ Low\ CO2\ Concentration$$

*ELSE (Zone Air CO2 Concentration $\geq$ Indoor High CO2 Concentration)*

$$VAV\ Minimum\ Airflow\ Fraction = Fraction\ at\ High\ CO2\ Concentration$$

*ELSE (Indoor Low CO2 Concentration $<$ Zone Air CO2 Concentration $<$ Indoor High CO2 Concentration)*

$$VAV\ Minimum\ Airflow\ Fraction = (10--(\frac{Zone\ Air\ CO2\ Concentration - Indoor\ Low\ CO2\ Concentration}{Indoor\ High\ CO2\ Concentration - Indoor\ Low\ CO2\ Concentration}) \times$$
$$(Fraction\ at\ High\ CO2\ Concentration - Fraction\ at\ Low\ CO2\ Concentration)$$

*END*

**Fig. 5** $CO_2$-Based control logic

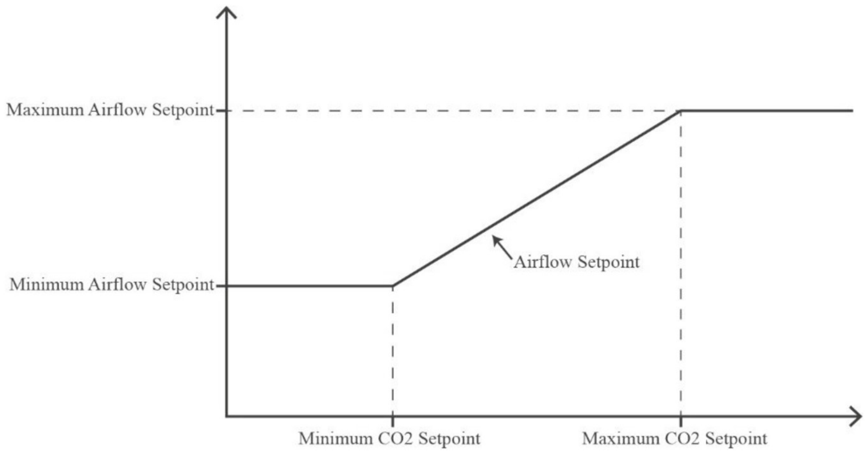


**Fig. 6** Suggested control logic

**Table 3** AHU Fan specification

| | Bottom floor | Middle floor | Top floor |
|---|---|---|---|
| Fan efficiency | 56% | | |
| Pressure rise | 1020 Pa | | |
| Maximum flow | 6.2 $m^3 \cdot s^{-1}$ | 6.7 $m^3 \cdot s^{-1}$ | 6.9 $m^3 \cdot s^{-1}$ |

fraction in accordance with $CO_2$ guidelines. A graphical representation is shown in Fig. 6.

The fan operation schedule in the HVAC system applied to the simulation model is depicted in Fig. 8 [47]. The direct expansion (DX) coil and heating coil operate continuously. The boiler and AHU gas heating coil directly use gas. Information regarding the boiler and coils is shown in Tables 3, 4, 5, 6.

$CO_2$ setpoint values for the DCV case and $CO_2$-Based case, referring to ASHRAE Standard 62.1 and California Title 24, respectively, are shown in Table 7.

**Table 4** Boiler specification

| Category | Value | |
|---|---|---|
| Capacity | 640 kW | |
| Nominal thermal efficiency | 78% | |
| Part load ratio | Minimum | 0 |
| | Maximum | 1.2 |
| | Optimum | 1 |
| Water outlet temperature upper limit | 95C° | |

**Table 5** AHU gas heating coil information

| Category | Value | |
|---|---|---|
| Efficiency | 80% | |
| Nominal capacity | Bottom floor | 53 kW |
| | Middle floor | 47 kW |
| | Top floor | 46 kW |

**Table 6** AHU DX coil specifications

| Category | | Bottom floor | Middle floor | Top floor |
|---|---|---|---|---|
| Cooling capacity | High speed | 138 kW | 143 kW | 147 kW |
| | Low speed | 46 kW | 48 kW | 49 kW |
| Air flow rate | High speed | 6.2 $m^3 \cdot s^{-1}$ | 6.7 $m^3 \cdot s^{-1}$ | 6.9 $m^3 \cdot s^{-1}$ |
| | Low speed | 2.1 $m^3 \cdot s^{-1}$ | 2.3 $m^3 \cdot s^{-1}$ | 2.2 $m^3 \cdot s^{-1}$ |
| Sensible heat ratio | High speed | 0.73 | 0.74 | 0.75 |
| | Low speed | 0.69 | | |
| COP | | 2.63 | | |

**Table 7** Default $CO_2$ setpoints per ASHRAE Standard 62.1—Office buildings [49]

| Occupancy category | $CO_2$ Setpoint [ppm] |
|---|---|
| Office space | 894 |
| Reception areas | 1656 |
| Telephone/data entry | 1872 |
| Main entry/lobbies | 1391 |

Considering that the simulation model is designed for an office building, reference values for office spaces were applied.

Furthermore, outdoor $CO_2$ concentration was set to 400 ppm [49], and the $CO_2$ setpoint value for zones(Conference Room) not covered by ASHRAE Standard 62.1 was 1000 ppm, following California Title 24 $CO_2$ setpoint guidance [48].

**Table 8** Internal heat gain [44]

| Category | Value | |
|---|---|---|
| People | Open office | 0.071person $m^{-2}$ |
| | Enclosed office | 0.077person $m^{-2}$ |
| | Conference room | 0.269person $m^{-2}$ |
| Lights | Open office<br>Enclosed office | 11.8W$m^{-2}$ |
| | Conference room | 14.0W$m^{-2}$ |
| Electric equipment | Open office | 13.8W$m^{-2}$ |
| | Enclosed office | 12.4W$m^{-2}$ |
| | Conference room | 14.3W$m^{-2}$ |

**Table 9** Infiltration [44]

| Type (refer to Fig. 1) | Value | |
|---|---|---|
| Enclosed office | Zone 1 and 2 | 2.10 ACH |
| | Zone 3 and 4 | 1.52 ACH |
| Conference room | 2.53 ACH | |

Table 8 and Table 9 present the values of internal heat gain and infiltration, respectively [50].

A scheduling graph for internal heat gain and infiltration is shown in Figs. 7, 8, 9 [51].

# 3 Results Analysis and Discussion

## 3.1 Minimum Airflow Fraction and $CO_2$ CONCENTRATION Relationship

Figures 10, 11, 12 illustrate the relationship between $CO_2$ concentration and the minimum airflow fraction in the CO2-based case, applying the control logic proposed in the study. In certain graphs depicting conference room and open office results, the red line denotes the room-specific maximum $CO_2$ setpoint detailed in the previous section.

Open office results are depicted in Fig. 10 (zones unaffected by infiltration). In zone 1 and 2 on the middle and top floors, $CO_2$ level approached or slightly exceeded the maximum $CO_2$ setpoint of 894 ppm. The reason why the bottom 1 and 2 zone exhibited higher $CO_2$ concentrations than the middle and top floor zones was that the bottom floor had a lower maximum airflow from the AHU fan compared to the other two floor levels.

For the enclosed office, results are presented in Fig. 11. In the graph, the enclosed office space remains within the maximum $CO_2$ setpoint of 894 ppm. However, zone 3 and 4 of bottom floor, as well as zone 3 of the middle and top floor, exhibit higher

$CO_2$ concentrations than zone 1 and 2 of all floors.

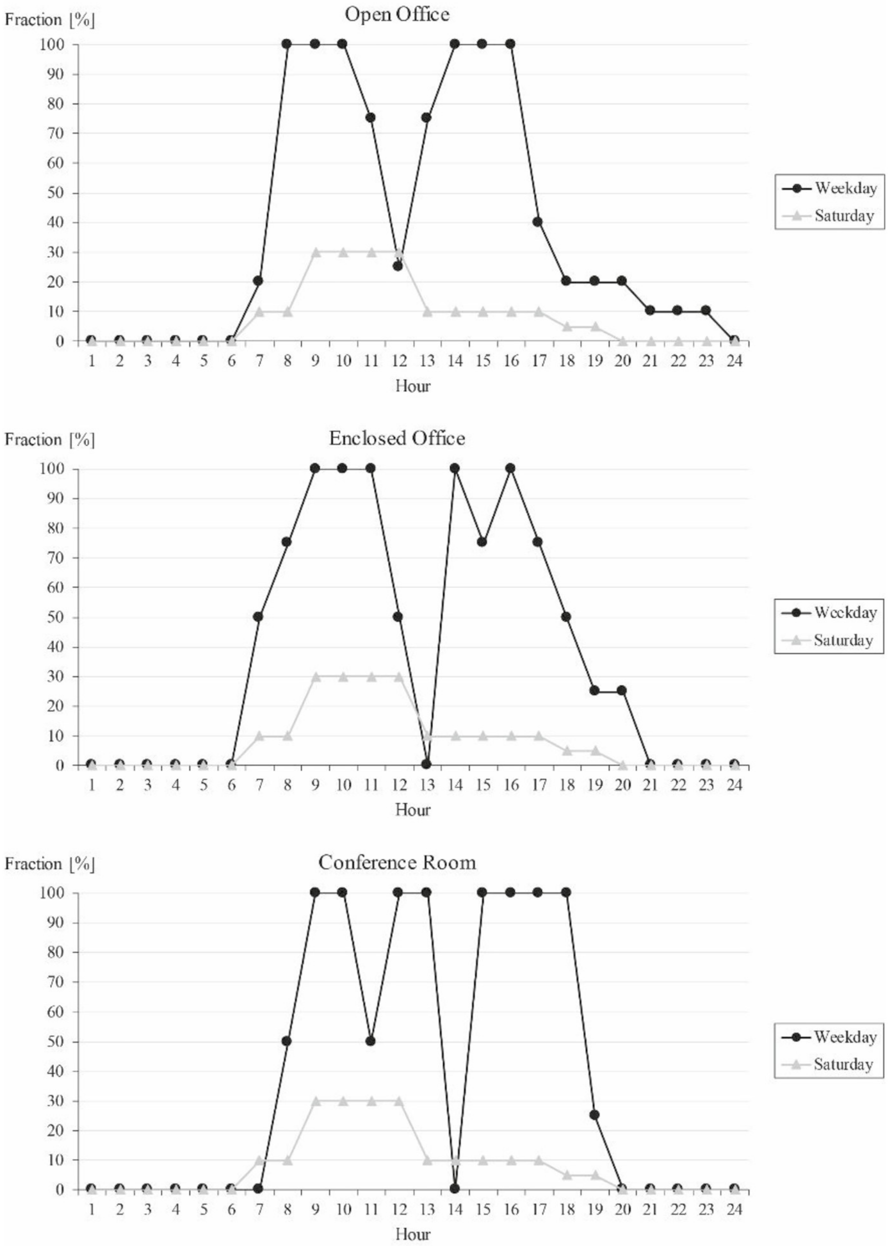


**Fig. 7** Occupancy schedule [44]

This difference in $CO_2$ concentration is due to different zone floor area, which, in turn, caused the difference in the maximum airflow rate. Specifically, zones 3 and 4 have smaller floor areas compared to zones 1 and 2 in each floor and thus zones 1

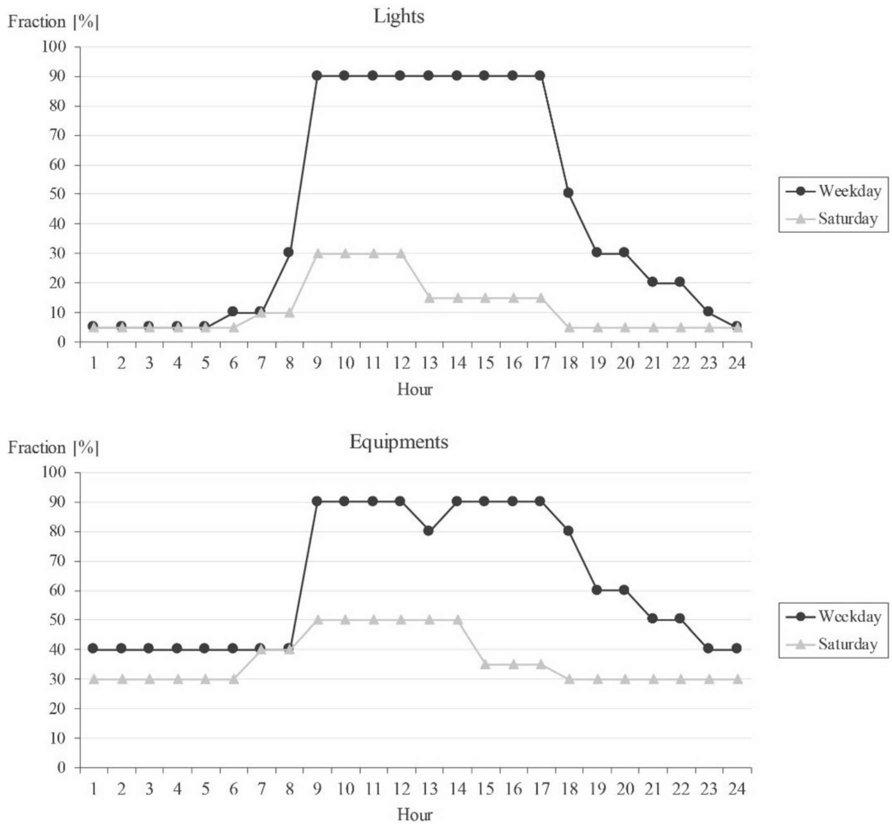


**Fig. 8** Lights and Equipment schedule [44]

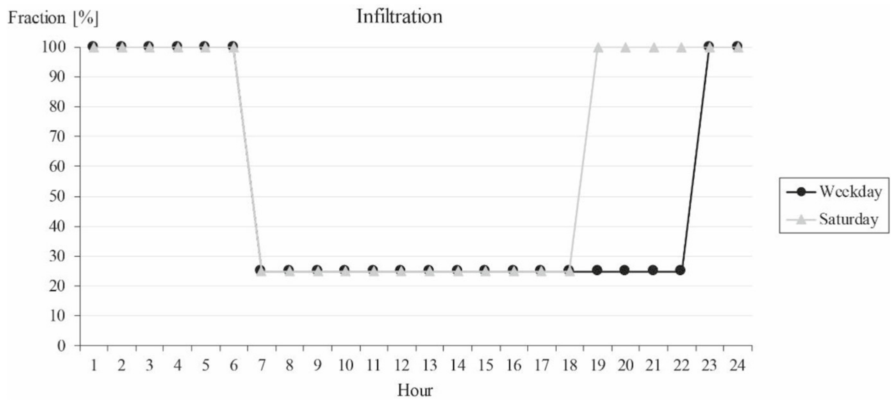


**Fig. 9** Infiltration schedule [44]

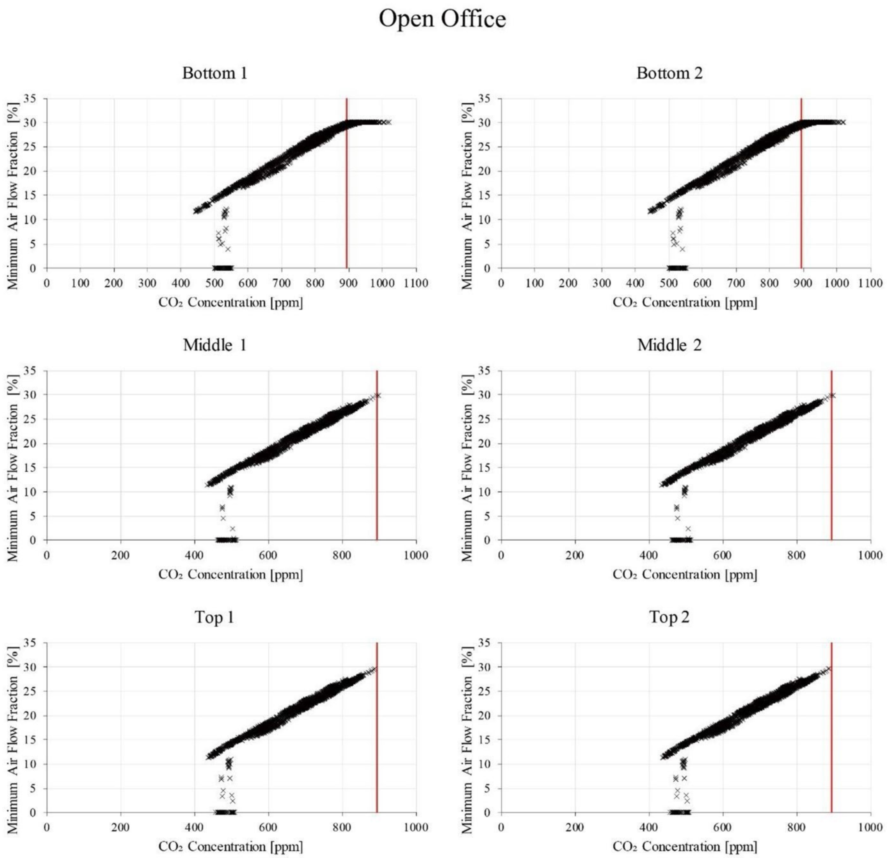


**Fig. 10** $CO_2$ concentration vs. minimum airflow fraction—Open office

and 2 had 78% lower maximum airflow rate, which is the number averaged over the entire cases.

Results for the conference room are presented in Fig. 12. According to the graph, in the case of the conference room, zone 1 and 2 located at the bottom, middle, and top floors share the same input conditions and do not exceed the maximum $CO_2$ setpoint of 1000 ppm, except for zone 1 and 2 at the bottom floor. In contrast, unlike the middle and top floors, the bottom 1 and 2 zone are found to be close to the maximum $CO_2$ setpoint for the conference room.

This is because, in a conference room with the same area, the maximum airflow rates of the fans covering the two zones of the bottom floor and the fans covering the middle and top zones differ. The outdoor airflow fraction of the two zones on the bottom floor is approximately 10% lower than that of the middle and top floors in the section with $CO_2$ concentration above 900 ppm.

The key points in this part are summarized as follows. Zones affected by infiltration did not exceed the $CO_2$ setpoint even with a lower airflow rate from the AHU

Enclosed Office

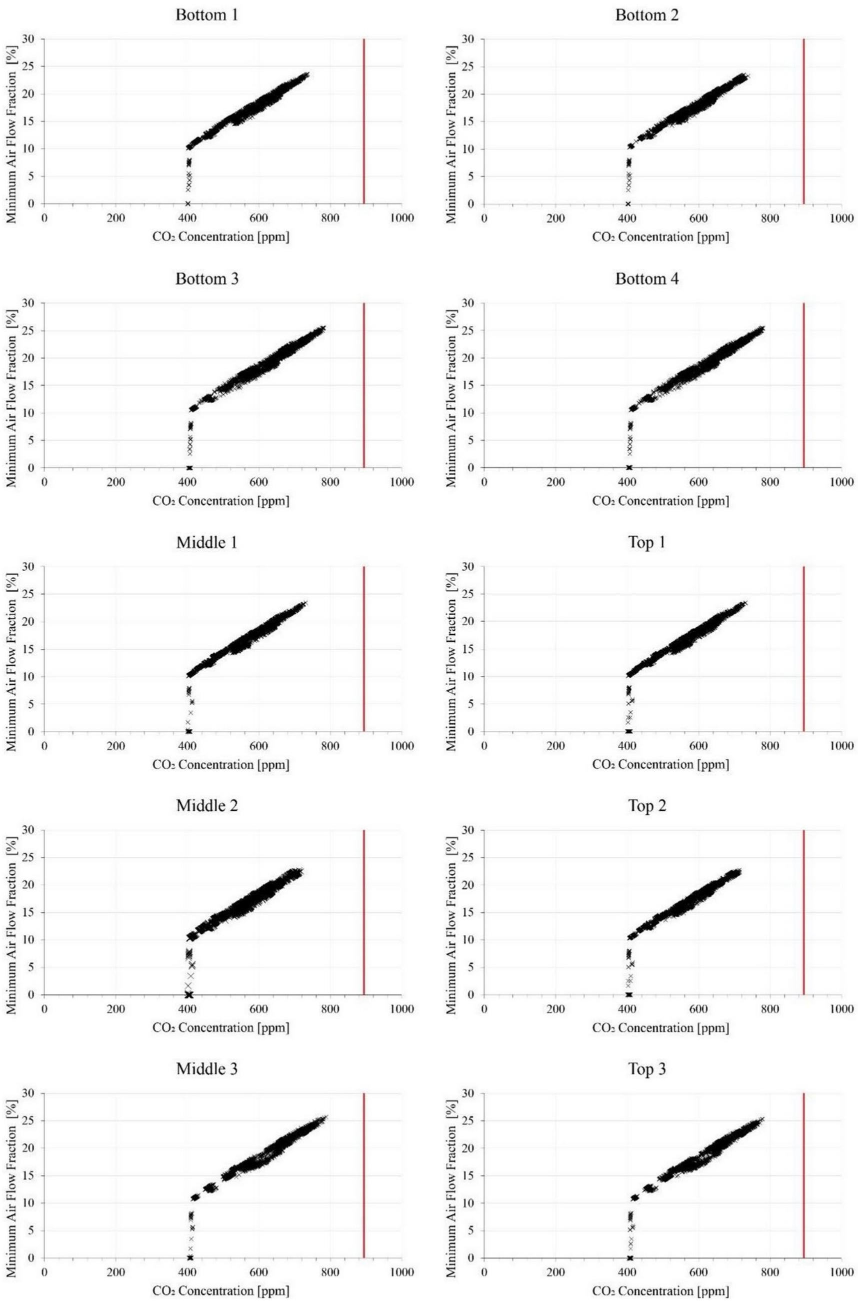

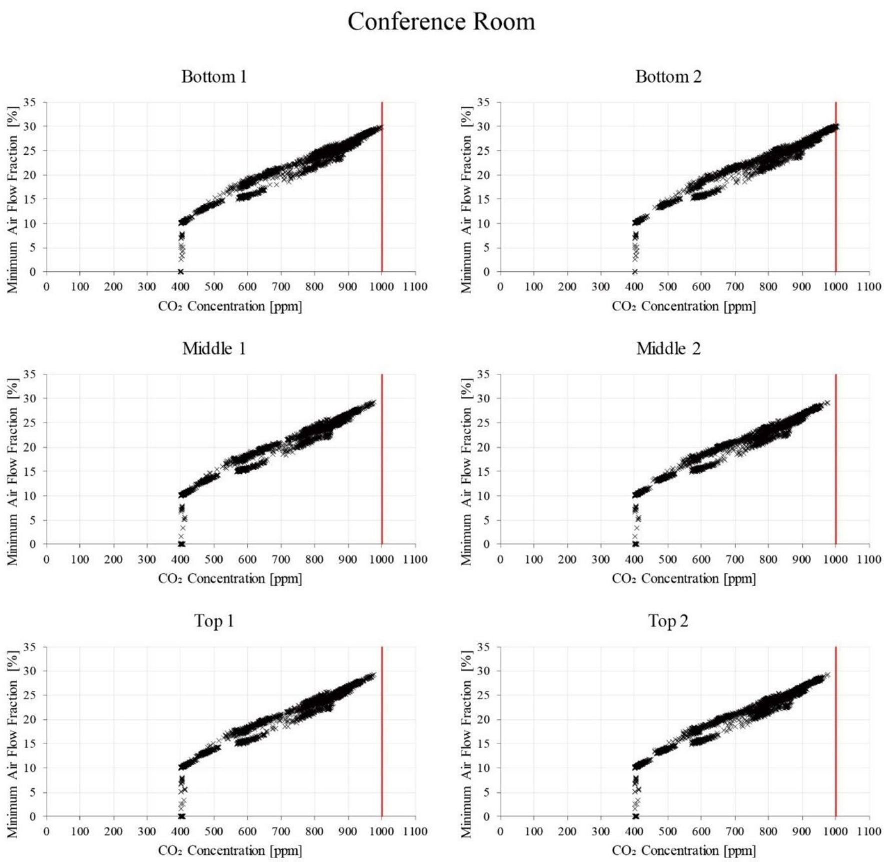


**Fig. 12** $CO_2$ concentration vs. minimum airflow fraction—Conference room

fan (in the case of the enclosed office and conference room). However, the zones that do not have enough infiltration and adequate airflow rate from the AHU fan will have high $CO_2$ concentration (in the case of the open office bottom 1 and 2 zone). Therefore, if the method suggested in the study is applied in a zone where there is no effect of infiltration and the fan airflow rate is low, the indoor $CO_2$ concentration may remain high, so appropriate measures such as increasing the fan airflow rate are necessary.

The following graphs (Figs. 13, 14, 15, 16, 17) illustrate the CO2 concentration and minimum airflow fraction in the VAV box for zones with a maximum $CO_2$ set-point of 1391 ppm, without infiltration.

Figure 13 presents the results for the Lobby and Dining, the only occupied spaces among the analyzed zones. However, since these areas are not primarily intended for continuous occupancy due to the building's function, the CO2 set-point was set at 1391 ppm. In the Lobby, a distinct pattern is observed on the bottom fl compared to the middle and top fl . Due to diff ences in VAV

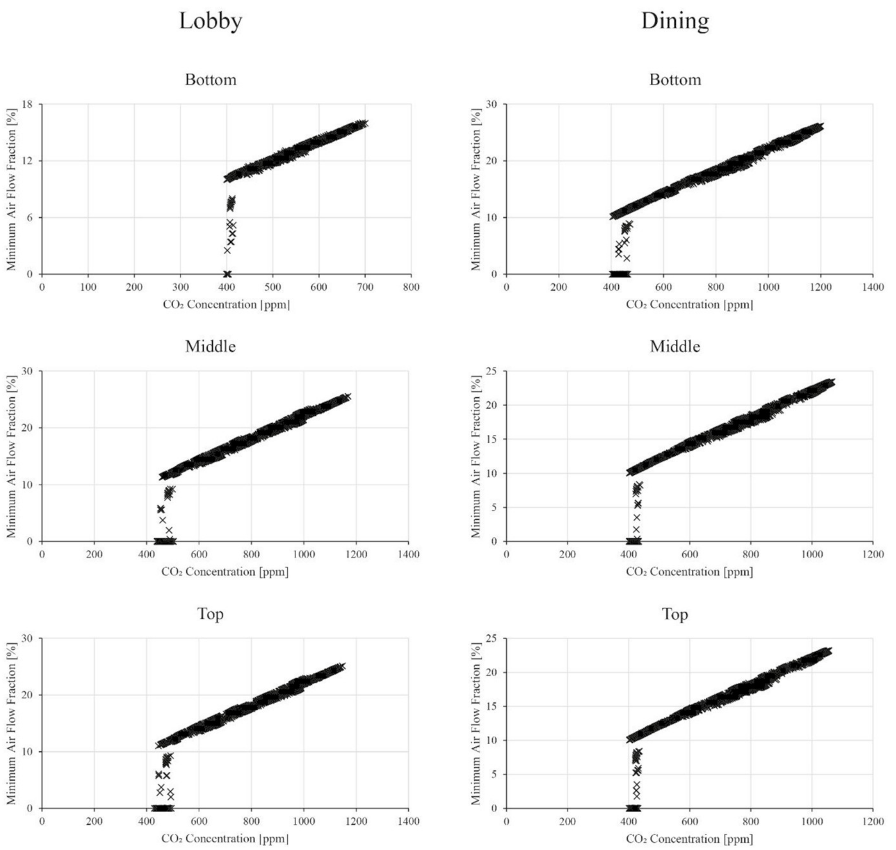


**Fig. 13** $CO_2$ concentration vs. minimum airflow fraction—Lobby and dining

box airfl w rates, $CO_2$ concentration on the bottom fl peaks at approximately 700 ppm, whereas on the middle and top fl it rises to around 1200 ppm. In the Dining zone, the lowest airfl w on the bottom fl leads to a maximum $CO_2$ concentration of 1200 ppm, while similar airfl w rates on the middle and top fl result in comparable $CO_2$ concentrations. In both zones, the $CO_2$ concentration does not exceed the setpoint of 1391 ppm.

Figure 14 presents the results for the Active Storage zones. Although 1–3 zone and 4 zone diff in size, a consistent pattern emerged across all zones. Zone 1 is the largest, zone 2 and 3 are of equal size, and zone 4 is the smallest. As all zones are unoccupied, a uniform $CO_2$ concentration pattern was observed. Regardless of zone size, the factors aff $CO_2$ concentration fl remained similar, leading to comparable results across the zones.

Figure 15 shows the results for the Corridor. Although these zones are adjacent to areas aff by infi ation, $CO_2$ concentration results were similar across fl Since there are no occupants and only minor variations in VAV box airfl w

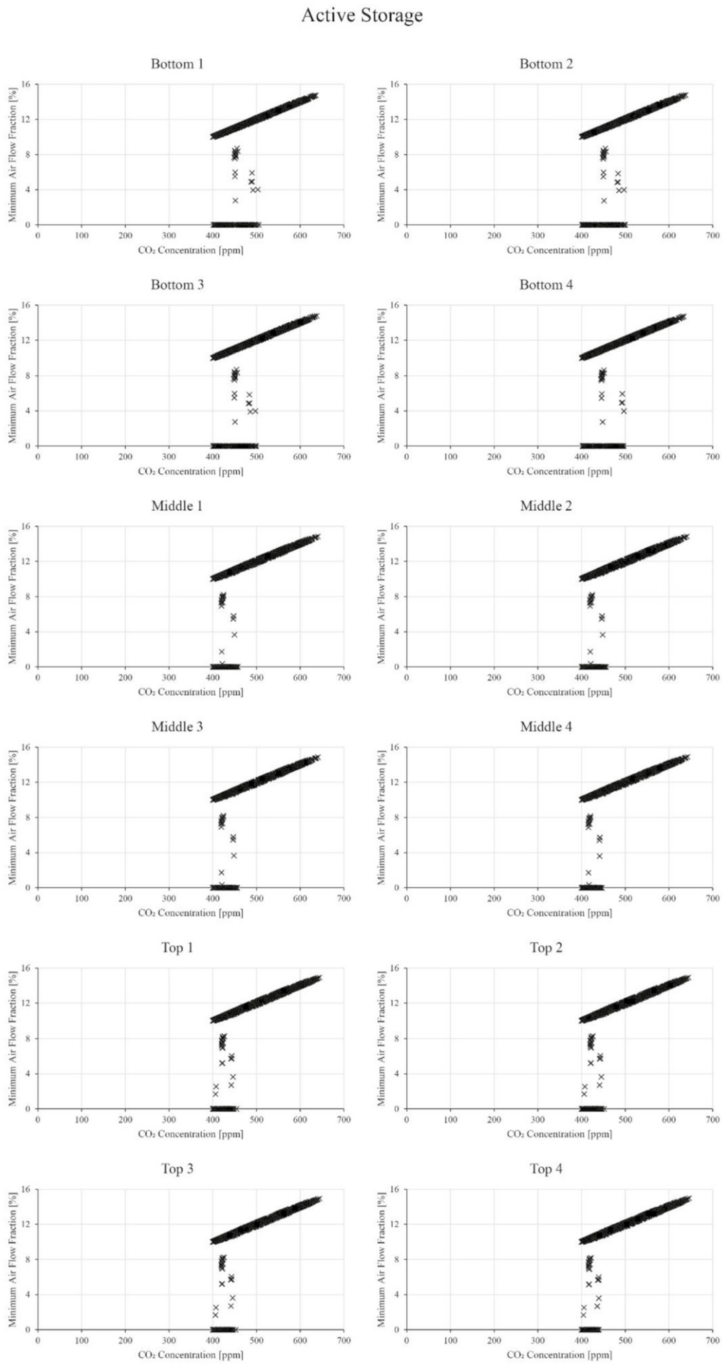


**Fig. 14** $CO_2$ concentration vs. minimum airflow fraction—Active storage

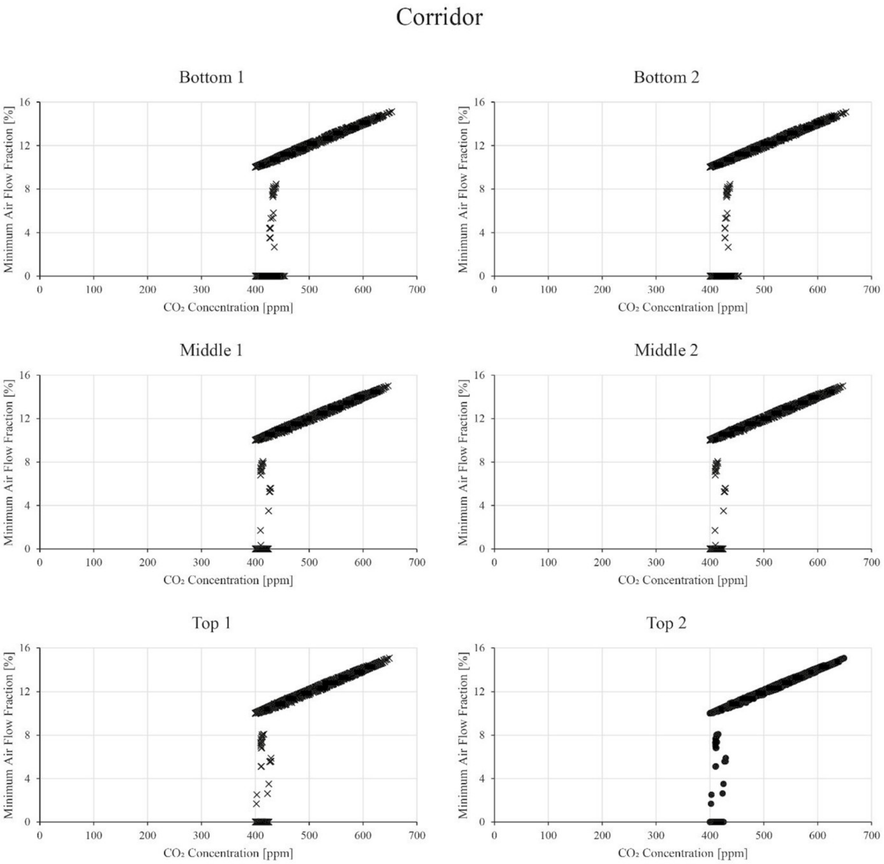


**Fig. 15** $CO_2$ concentration vs. minimum airflow fraction—Corridor

rates between fl other infl factors are minimal, leading to consistent $CO_2$ concentration outcomes across all levels.

Figure 16 presents the results for the Mechanical and Restroom. Both zones are unoccupied spaces, and while airflow rates differ between the bottom floor and the middle and top floors, the factors influencing $CO_2$ concentration are consistent across floors. As a result, similar $CO_2$ concentration outcomes are observed throughout these zones.

Figure 17 presents the results for the Stair. Each floor contains two stair zones, and, like the other zones, these zones are unoccupied spaces. Although airflow rates vary between the bottom and middle/top floors, the factors influencing $CO_2$ concentration are similar across floors, resulting in consistent outcomes.

The key points in this part are summarized as follows. In the Lobby, the bottom floor showed a lower CO2 concentration compared to the middle and top floors, which was due to differences in the airflow from the VAV box. In the Dining, the bottom floor exhibited the lowest airflow, resulting in a $CO_2$ concentration of

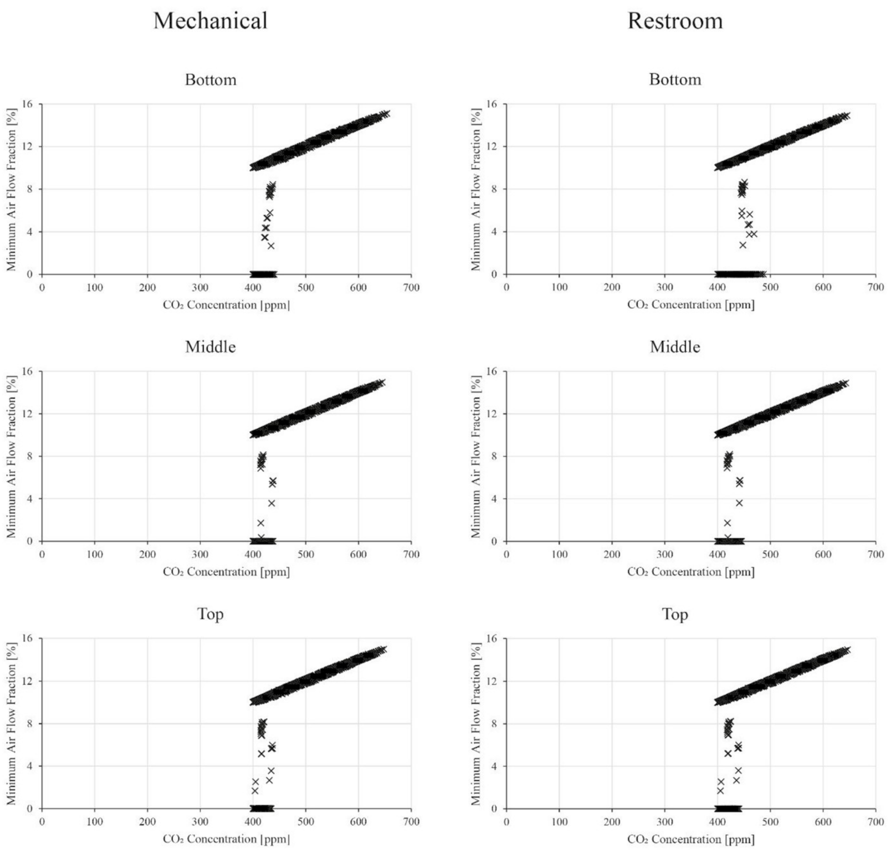


**Fig. 16** CO2 concentration vs. minimum airflow fraction—Mechanical and restroom

1200 ppm, while the middle and top floors had similar $CO_2$ levels due to similar airflow. Both zones did not exceed the $CO_2$ setpoint. For the Active Storage, Mechanical and Restroom, Stair, and Corridor, which are non-occupied spaces, the results were consistent across floors due to similar airflow conditions, regardless of zone size or floor. For this reason, increasing the airflow rate is essential for controlling $CO_2$ levels in spaces with low ventilation.

## 3.2CO2 Concentration

The presented results depict $CO_2$ concentrations in various simulation cases summarized in Table 2, where the control logic proposed in this study regulates the minimum airflow fraction of the installed VAV box in each zone. In the control logic, since this fraction is associated with the heating season, the hourly $CO_2$ concentration was analyzed for specific days during the heating season. The analysis is of the

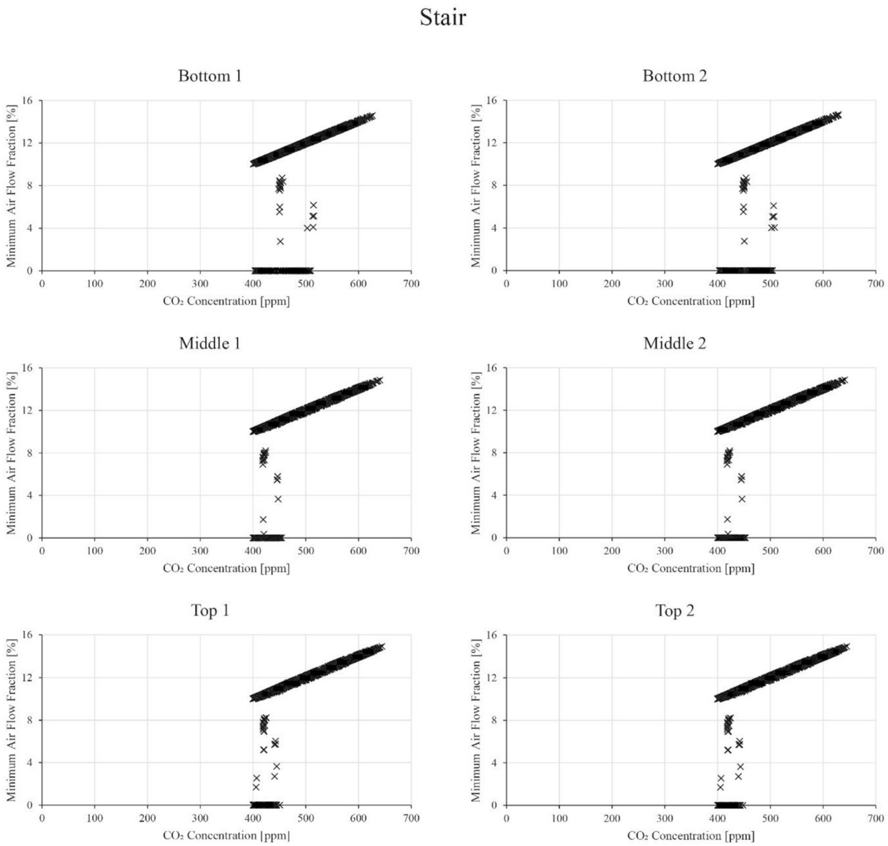


**Fig. 17** $CO_2$ concentration vs. minimum airflow fraction—Stair

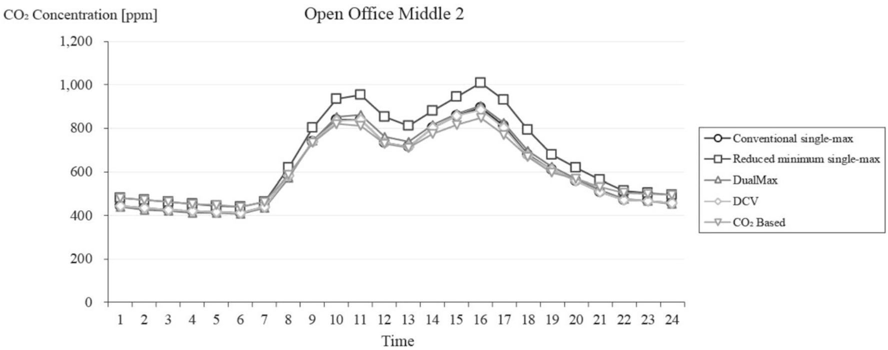


**Fig. 18** Hourly $CO_2$ concentration(Jan 25)—Open office

hourly $CO_2$ concentration on Wednesday, January 25 for the open office, enclosed office, and conference room located on the middle floor.

Beginning with the open office zone, 2 zone with the largest areas were selected. Figure 18 illustrates that reduced minimum single-max exhibits the highest concentration pattern during occupied times, surpassing the ASHRAE-recommended $CO_2$ concentration for office space (894 ppm) for most of the occupied time. This is followed by the conventional single-max, DualMax, and DCV groups. The $CO_2$-Based control logic in this study demonstrates a similar $CO_2$ concentration level as reduced minimum single-max during non-occupancy hours, with the lowest concentration during occupancy hours. In the $CO_2$-Based case, the minimum airflow fraction increases proportionally with the rising $CO_2$ concentration during occupancy. Conversely, the reduced minimum single-max case, fixed at 15% during occupied hours, does not mitigate the increasing $CO_2$ concentration.

Moving to Fig. 19 for the enclosed office, results indicate that reduced minimum single-max has the lowest $CO_2$ concentration during occupied hours, contrasting with the open office results. The $CO_2$-Based case has the highest concentration, followed by the conventional single-max and DCV cases, with the DualMax case slightly higher than the conventional single-max and DCV. This discrepancy is likely due to the fact that the reduced minimum single-max scenario has the highest outdoor airflow supplied to the zone by the terminal unit during the system operation time.

Figure 20 displays the conference room results, mirroring the open office findings. The reduced minimum single-max case exhibits the highest $CO_2$ concentration during occupancy, while the $CO_2$-Based case shows the lowest. The conventional single-max, DualMax, and DCV cases display similar $CO_2$ concentrations and patterns. This is because the minimum airflow fraction is high among the factors to maintain proper indoor air quality, and in the $CO_2$-Based case, the minimum airflow fraction was set appropriately according to the hourly $CO_2$ concentration, resulting in the lowest $CO_2$ concentration among the cases.

In Fig. 21, the annual hourly average $CO_2$ concentration for occupied zones from 07:00 to 22:00 on weekdays is presented. Reduced minimum single-max case

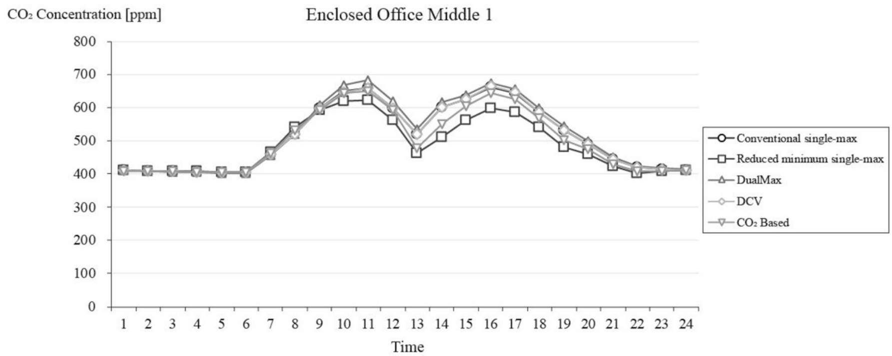


**Fig. 19** Hourly $CO_2$ concentration(Jan 25)—Enclosed office

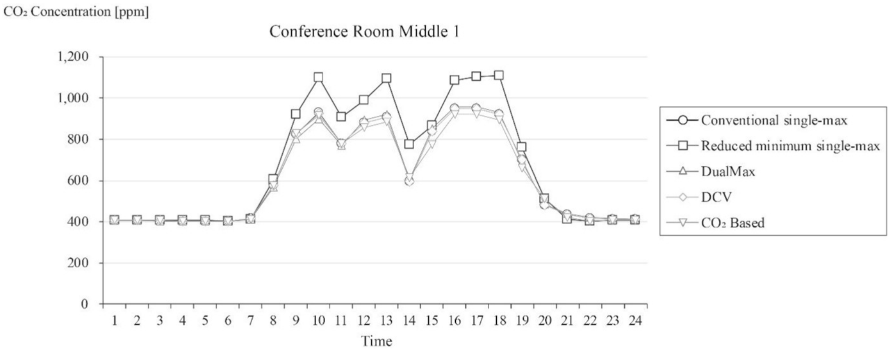


**Fig. 20** Hourly $CO_2$ concentration(Jan 25)—Conference room

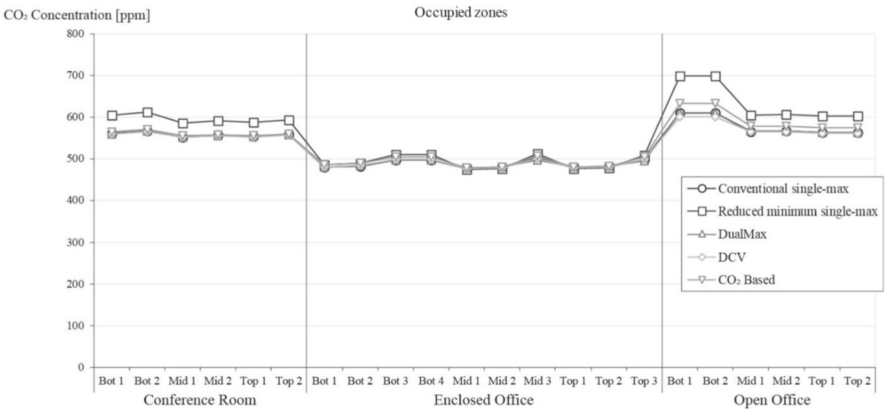


**Fig. 21** Annual hourly average $CO_2$ concentration—Target zones

shows higher concentrations than the other cases in the conference room, while the enclosed office exhibits no significant difference. However, in the open office, substantial differences exist between zones 1 and 2. In middle floor zone 1 and 2 and top floor zones 1 and 2, the reduced minimum single-max case has a higher average $CO_2$ concentration than the other cases. Additionally, the $CO_2$-Based case has a slightly higher average $CO_2$ concentration than the other three scenarios in these zones. This is because the bottom floor zone 1 and 2 have the largest open office space areas, but the maximum airflow rate is lower than that of fans on the other two floors. The average minimum airflow fraction in the reduced minimum single-max case is much lower than in the other cases, resulting in a higher average $CO_2$ concentration.

## 3.3 Heating Supply and Heating Energy Consumption

Figure 22 illustrates the heating supply from the reheat coils for each space type. Heating supply was proportional to the capacity of each reheat coil. In the bottom

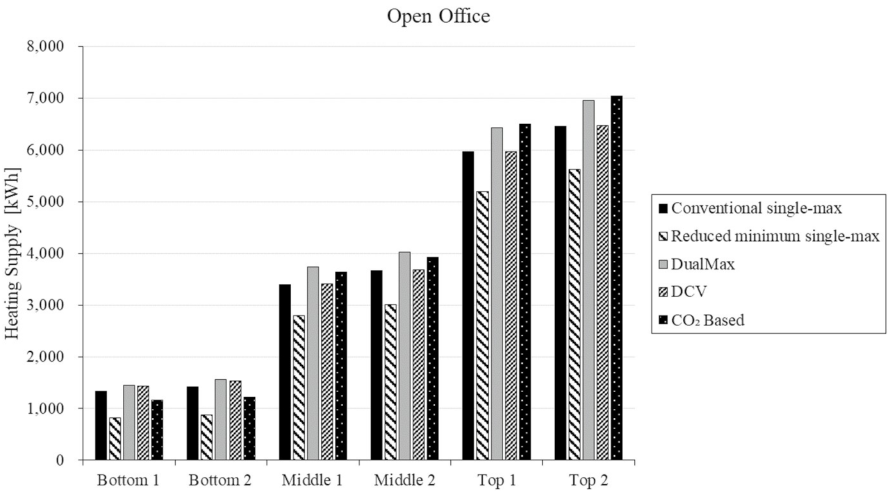


**Fig. 22** Reheat coil heating supply—Open office

zones of the open office, which displayed a higher average $CO_2$ concentration in the previous section, heating supply is lower than in middle and top zones. In the bottom zones, where the heating supply scale is relatively small, the reduced minimum single-max case has the smallest heating supply, while depending on the floor, DualMax is the largest (bottom and middle), or $CO_2$ Based is the largest (top). Conversely, the heating supply for the conventional single-max and DCV cases was lower than those of DualMax and $CO_2$ Based as the floor level increased. The reduced minimum single-max case had the lowest heating supply across all the floor levels.

In the enclosed office (Fig. 23), similar to the result observed in the open office, heating supply of each zone was proportional to the capacity of the reheat coil. In

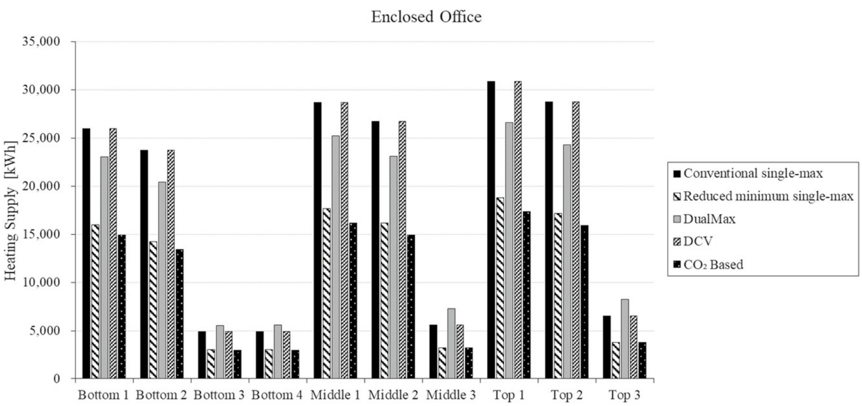

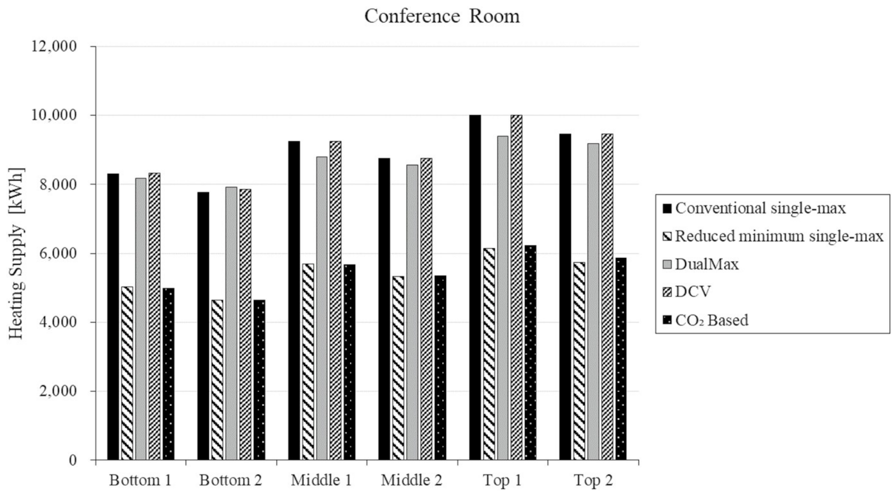


**Fig. 24** Reheat coil heating supply—Conference room

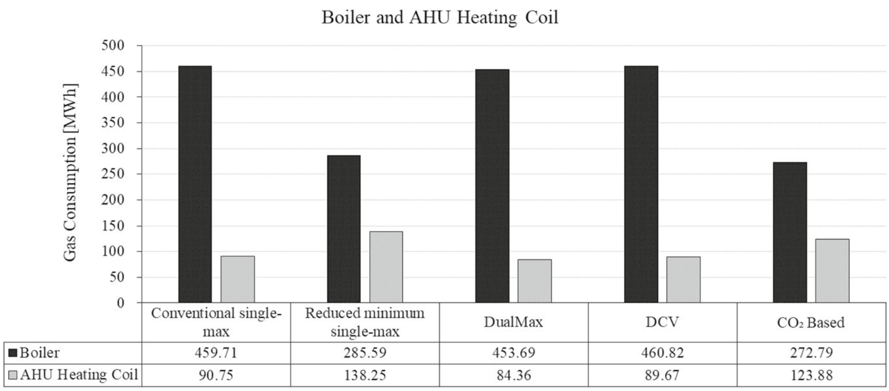


**Fig. 25** Boiler and AHU gas heating coil energy consumption

contrast to zones 1 and 2, where the heating supply is high, the heating supply of the DualMax case is the highest in zone 3 and 4. In zone 1 and 2, the DCV case is similar to the conventional single-max case, and the heating supply increases in the order of the DualMax case, reduced minimum single-max case, and $CO_2$-Based case. Particularly, the difference in heating supply between the $CO_2$-Based and reduced minimum single-max cases is larger in the enclosed office results than in the open office results.

Figure 24 presents the heating supply results for the conference room. For the conference room, the conventional single-max and DCV cases exhibit similar values, followed by the DualMax, reduced minimum single-max, and $CO_2$-Based cases. However, in bottom 2 zone, DualMax has the highest heating supply. In the

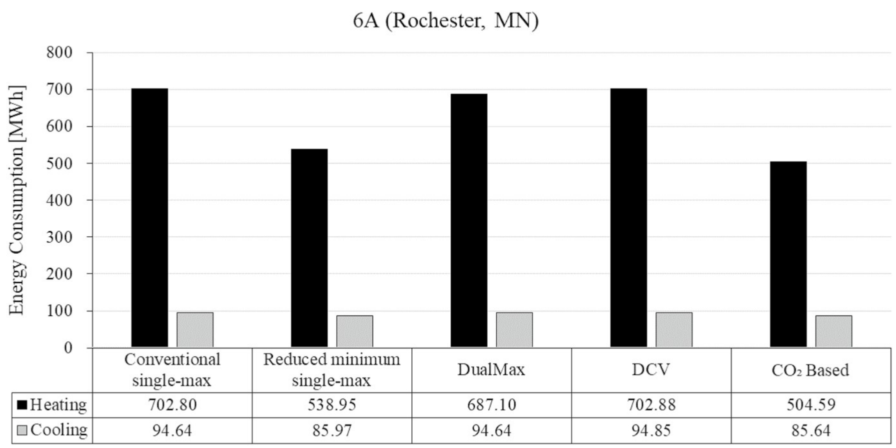


**Fig. 26** Cooling and heating energy consumption—6A(Rochester, Minnesota)

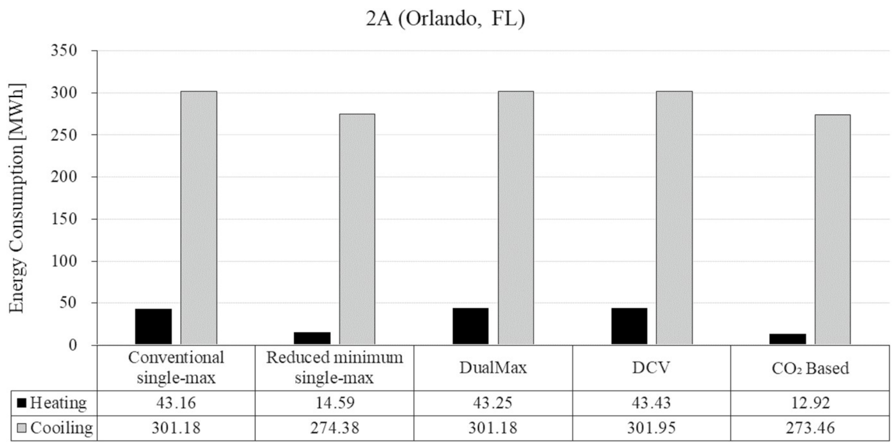


**Fig. 27** Cooling and heating energy consumption—2A(Orlando, Florida)

conference room, the heating supply in the $CO_2$-Based case is higher than that in the reduced minimum single-max case.

Figure 25 shows the total gas consumption of the boiler supplying hot water to the reheat coils and three AHU gas heating coils. Similar to the results of the previous reheat coil heat supply, the gas consumptions of the DCV, conventional single-max, and DualMax cases are similar, followed by the reduced minimum single-max case and $CO_2$-Based case. It is also observed that the lower the boiler gas consumption, the higher the AHU gas heating coil gas usage, as the room temperature is lower due to the lower airflow rate, requiring more heating than in other cases. Specifically, the two cases with higher AHU gas heating coil gas consumption have an average indoor temperature about 0.5 degrees lower than the other three cases during the heating season, excluding weekends.

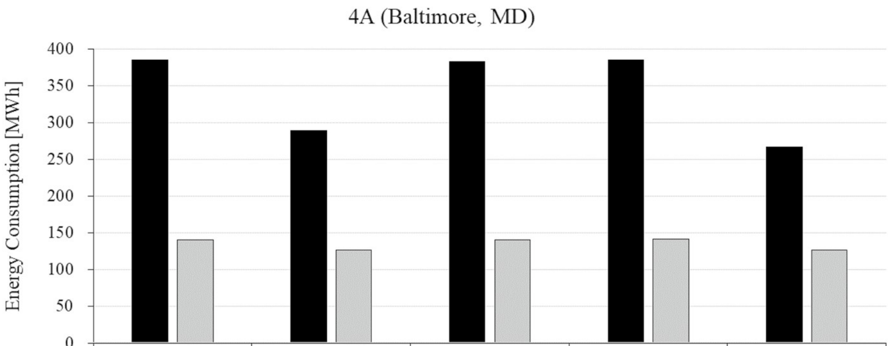


| | Conventional single-max | Reduced minimum single-max | DualMax | DCV | $CO_2$ Based |
|---|---|---|---|---|---|
| ■ Heating | 384.77 | 288.79 | 383.05 | 385.01 | 267.09 |
| □ Cooiling | 140.66 | 126.58 | 140.67 | 140.99 | 126.43 |

**Fig. 28** Cooling and heating energy consumption—4A(Baltimore, Maryland)

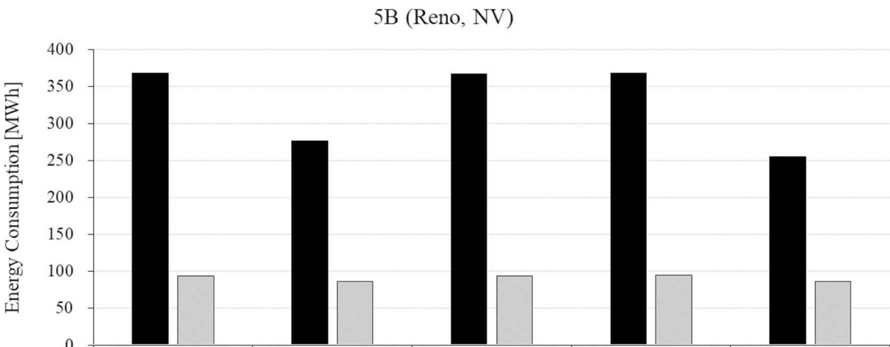


| | Conventional single-max | Reduced minimum single-max | DualMax | DCV | $CO_2$ Based |
|---|---|---|---|---|---|
| ■ Heating | 367.75 | 276.30 | 366.77 | 368.00 | 255.45 |
| □ Cooiling | 94.04 | 85.89 | 94.04 | 94.27 | 85.98 |

**Fig. 29** Cooling and heating energy consumption—5B(Reno, Nevada)

### 3.4Heating and Cooling Energy Consumption

Figures 26, 27, 28, 29 depict a graph illustrating the total cooling(electricity) and heating(gas) energy consumption in climate zone 6A(cold humid), 2A(hot humid), 4A(mixed humid), and 5B(cool dry) [43]. Heating and cooling energy includes DX coil electricity, boiler gas, and AHU gas heating coil gas usage. The cooling energy consumption is the aggregate of the AHU DX coils' energy consumption installed from the bottom floor to the top floor. Meanwhile, heating energy consumption encompasses the total gas usage of the boiler and three AHU gas heating coils, as detailed in the preceding section.

In Fig. 26, there was no significant disparity in cooling energy consumption among the three cases (conventional single-max, dualmax, and DCV) with a minimum airflow fraction of 30%. Conversely, both the reduced minimum single-max case and the $CO_2$-based control proposed in this study exhibited approximately 10 MWh(about 9%) lower consumption than the three cases collectively. Moreover, the $CO_2$-based control was approximately 0.3 MWh(about 0.4%) lower than the reduced minimum single-max case. Since the minimum airflow fraction mainly affects the heating loop, it is expected that the control method proposed in this study can reduce energy in the cooling season in addition to the heating season if the parameter is adjusted appropriately for the cooling season.

Concerning heating energy consumption, the three cases with a minimum airflow fraction of 30% displayed no significant differences, mirroring the findings in the cooling section. Both the reduced minimum single-max and $CO_2$-Based cases, show- casing lower values in the heating energy section, demonstrated an approximately 30% reduction in heating energy consumption compared to the other three cases. In both instances, the boiler energy consumption was lower, and the total AHU gas heating coil energy consumption was higher than in the other cases. However, the energy consumption scale of the AHU gas heating coil was smaller than that of the boiler, resulting in a similar pattern of results. When comparing the reduced mini- mum single-max and $CO_2$-Based cases, the $CO_2$-Based case exhibited the lowest heating energy consumption among the five cases, approximately 30 MWh (about 6%) lower than that of the reduced minimum single-max case.

In Fig. 27, the proportion of cooling energy consumption exceeded that of heating energy consumption, consistent with the characteristics of the climate zone (hot and humid). There was no significant difference in cooling energy consumption except for variations between the three cases(conventional single-max, DualMax, and DCV) with a minimum airflow fraction of 30% and the two cases(reduced minimum single-max and $CO_2$ based) with a lower minimum airflow fraction. The disparity in cooling energy consumption between the two groups was around 9%. Similar trends were observed in heating energy consumption, with the $CO_2$-based case registering approximately 70% lower than the three cases(conventional single-max, DualMax, and DCV) with a minimum airflow fraction of 30%, and 11% lower compared to the reduced minimum single-max case. Hence, the necessity for a control method enabling energy savings, particularly in regions with a high cooling energy propor- tion like the corresponding climate area, was confirmed. The reasoning behind this is that the proportion of cooling energy is substantial, yet the reduction in cooling is minimal, while the reduction in heating is significant.

In Figs. 28 and 29, the energy consumption results for climate regions 4A and 5B exhibited similarities. Particularly, heating consumption was nearly identical, but there was a discrepancy in cooling consumption. This discrepancy appears to stem from differences between mixed and cool climate regions. Upon closer examination, in terms of heating energy consumption, the $CO_2$-based case was 30% lower than the three cases(conventional single-max, DualMax, and DCV) where the minimum airflow fraction was 30% in both 4A and 5B. For cooling energy consumption, the $CO_2$-based case was about 10% lower than the three cases(conventional single-max, DualMax, and DCV) with a minimum airflow rate of 30% in 4A and about 5% lower in 5B. In both climate zone, the heating energy consumption of the $CO_2$-

based case  was approximately 8% lower than that of the reduced minimum single-max case, but cooling energy consumption remained almost the same. This outcome mirrors that of climate zone 6A, indicating a continued need for further enhancement of the control method to save cooling energy.

## 4 Conclusion

In this study, we explored the impact on IAQ and energy consumption of employing a linear control method to adjust the VAV minimum airflow fraction based on the specific maximum and minimum CO2 concentrations. EnergyPlus served as the primary tool, utilizing the inherent EMS function to implement the proposed control logic. The results are detailed below.

Initially, we scrutinized the correlation between CO2 concentration and minimum airflow fraction in the proposed control logic's simulation results. In the open office, differences in CO2 concentration among different floor levels occurred due to differences in outdoor airflow passing through each VAV unit. Regarding the conference room, the difference in outdoor airflow fraction caused a slight difference in CO2 concentration between the bottom floor and the two floors.

The analysis involved selecting one zone for each of the three space types and assessing hourly concentration on a specific day (Jan 25) and the average CO2 concentration during HVAC operating hours throughout the year. In the open office and the conference room's hourly concentration analysis, the CO2 concentration-based control logic achieved the lowest concentration during occupied hours. In the average CO2 concentration analysis, the open office indicated that the CO2-Based Case showed a slightly higher average CO2 concentration than the three lowest cases(conventional single-max, DualMax, and DCV).

In the analysis of heating energy consumption, we assessed the heating supply of the reheat coil, directly linked to the minimum airflow fraction by each space type, along with the gas consumption of the boiler supplying hot water to reheat coils. The examination of reheat coil heating supply in the open office zone group revealed that the heating supply of the reduced minimum single-max case and CO2-Based case was lower than the other three cases. However, the difference between the two cases increased with floor levels, and the CO2-Based case was lower than that of the reduced minimum single-max case. The boiler gas energy consumption was proportional to the minimum airflow fraction. CO2-Based case was the lowest at 272.79 MWh. Similarly, the cooling energy consumption, which is the sum of the DX coils installed in the three AHUs, turns out to be the lowest in the CO2-Based case at 85.64 MWh(in 6A climate zone). The proposed control method was observed to achieve savings of approximately 30% in heating and up to about 10% in cooling across four climate zones (2A, 4A, 5B, and 6A).

The study, using a linear control technique for VAV box minimum airflow, found that aligning the minimum airflow fraction in VAV box with CO2 concentration can reduce heating and cooling energy consumption while maintaining satisfactory indoor CO2 level. In contrast, since the research was conducted solely through simulations targeting building for specific purposes (office building), issues may arise when applied to actual buildings, including measurement errors due to sensor installation points and the number of sensors, as well as problems with transmitting sensor measurement data. In addition, as the study did not consider the extent of occupants' exposure to indoor CO2 concentrations, it is necessary to reflect on control methods that take into account the IAQ and health aspects of occupants by refining conditions by time (one or two hours) and CO2 concentration (1000 or 2000 ppm) while reducing energy use. In future studies, it is necessary to optimize the number and location of sensors for implementing control methods in actual buildings and to prepare countermeasures for data transmission issues that may arise in real-world situations. In addition, through scenarios involving various air pollutants, including CO2, particle matter, and volatile organic compounds, efforts should be made to implement control methods that have a positive impact on human health while maintaining appropriate IAQ.

**Acknowledgments** This work was supported by the Korea Institute of Energy Technology Evaluation and Planning (KETEP) and the Ministry of Trade, Industry & Energy (MOTIE) of the Republic of Korea (No. 20224000000560). This work was supported by the National Research Foundation of Korea(NRF) grant funded by the Korea government(MSIT) (No. RS-2023-00217322).

**Author Contributions** Jong Man Lee wrote original draft. Kwang Ho Lee did the funding acquisition. Jin Woo Moon did the data curation and analysis. Sang Hoon Lee and Tianzhen Hong extensively reviewed the paper.

**Data Availability** No datasets were generated or analyzed during the current study.

## Declarations

**Conflict of interest** The authors declare no competing interests.

## References

1. Intergovernmental Panel on Climate Change (IPCC). Summary for policymakers, in: climate change 2022: mitigation of climate change. Contribution of working group III to the sixth assessment report of the intergovernmental panel on climate change. (2022)
2. COP 26 in Glasgow. Editorial, Int. J. Refrigeration, 132, pp. 5–7. (2021)
3. Y. Liang, C. Li, Z. Liu, X. Wang, F. Zeng, X. Yuan, Y. Pan, Decarbonization potentials of the embodied energy use and operational process in buildings: a review from the life-cycle perspective. Heliyon **9**(10), e20190 (2023)
4. International Energy Agency (IEA). Technology and innovation pathways for zero-carbon-ready buildings by 2030. (2022)
5. J. Park, S.H. Hong, S.H. Yeon, B.M. Seo, K.H. Lee, Predictive Model for Solar Insolation Using the Deep Learning Technique, Int. J. Energy Res. **2023**, 3525651 (2023)
6. B. Seo, Y. Yoon, K.H. Lee and S. Cho, Comparative Analysis of ANN and LSTM Prediction Accuracy and Cooling Energy Savings Through AHU-DAT Control in an Office, Build. **13**, 1434 (2023)
7. G.S. Okochi, Y. Yao, A review of recent developments and technological advancements of variable-air-volume (VAV) air-conditioning systems. Renew. Sustain. Energy Rev. **59**, 784–817 (2016)
8. H.J. Jee, S.H. Yeon, J. Park, Y. Yoon, K.H. Lee, Machine learning based simultaneous control of air handling unit discharge air and condenser water temperatures set-point for minimized cooling energy in an office building. Energy Build. **297**, 113471 (2023)
9. J.M. Lee, S.H. Hong, B.M. Seo, K.H. Lee, Application of artificial neural networks for optimized AHU discharge air temperature set-point and minimized cooling energy in VAV system. Appl.

Therm. Eng. **153**, 726–738 (2019)

10. D. Kim, J. Lee, S. Do, P.J. Mago, K.H. Lee, H. Cho, Energy modeling and model predictive control for HVAC in buildings: a review of current research trends. Energies **15**(19), 7231 (2022)
11. J. Zhang, R.G. Lutes, G. Liu, M.R. Brambley. Energy savings for occupancy-based control (OBC) of variable-air-volume (VAV) systems. PNNL-22072, pp. 1–79, Virginia, The United States of America. (2013)
12. W. Wang, J. Zhang, M.R. Brambley, B. Futrell, Performance simulation and analysis of occupancy-based control for office buildings with variable-air-volume systems. Energies **13**(15), 3756 (2020)
13. F. Niu, Z. O'Neill, X. Zhou, D. Qian. Model-based optimal control of variable air volume terminal box. International High Performance Buildings Conference, 176. (2016)
14. S.G. Choi, J.U. Jeon, K.S. Kim, Evaluation of energy performance and indoor environment according to the VAV system control strategies. J. KIAEBS **12**(2), 130–147 (2018)
15. X. Ji, J. Li, T. Gao. Research on wavelet neural network decoupling control of variable-air-volume air-conditioning system. 2018 Chinese Control and Decision Conference (CCDC), pp. 1848–1853. (2018)
16. G. Feng, S. Lei, X. Gu, Y. Guo, J. Wang, Predictive control model for variable air volume terminal valve opening based on backpropagation neural network. Build. Environ. **188**, 107485 (2021)
17. H.J. Kim, Y.H. Cho, Optimization of supply air flow and temperature for VAV terminal unit by artificial neural network. Case Stud. Ther. Eng. **40**, 102511 (2022)
18. W. Li, S. Wang, C. Koo, A real-time optimal control strategy for multi-zone VAV air-conditioning systems adopting a multi-agent based distributed optimization method. Appl. Energy **287**, 116605 (2021)
19. X. Li, T. Zhao, J. Zhang, T. Chen, Predication control for indoor temperature time-delay using Elman neural network in variable air volume system. Energy Build. **154**, 545–552 (2017)
20. S. Ma, Y. Zou, S. Li, Coordinated control for air handling unit and variable air volume boxes in multi-zone HVAC system. J. Process. Control. **107**, 17–26 (2021)
21. N. Nasirpour, S. Balochian, Optimal design of fractional-order PID controllers for multi-input multi-output (variable air volume) air-conditioning system using particle swarm optimization. Intell. Build. Int. **9**(2), 107–119 (2016)
22. S. Rahnama, A. Afshari, N.C. Bergsøe, S. Sadrizadeh, Experimental study of the pressure reset control strategy for energy-efficient fan operation. Energy Build. **139**, 72–77 (2017)
23. S. Rahnama, A. Afshari, N.C. Bergsøe, S. Sadrizadeh, G. Hultmark, Experimental study of the pressure reset control strategy for energy-efficient fan operation—part 2: variable air volume ventilation system with decentralized fans. Energy Build. **172**, 249–256 (2018)
24. N.C. Seong, J.H. Kim, W. Choi, Optimal control strategy for variable air volume air-conditioning systems using genetic algorithms. Sustainability **11**, 5122 (2019)
25. Y. Zhang, T. Yan, X. Xu, J. Gao, G. Huang, Room temperature and humidity decoupling control of common variable air volume air-conditioning system based on bilinear characteristics. Energy Built Environ. **4**, 354–367 (2023)
26. X. Zhu, T. Shi, X. Jin, Z. Du, Multi-sensor information fusion based control for VAV systems using thermal comfort constraints. Build. Simul. **14**, 1047–1062 (2020)
27. Q. Meng, X. Yan, Q. Ren, Global optimal control of variable air volume air-conditioning system with iterative learning: an experimental case study. J. Zhejiang Univ.-Sci. A **16**(4), 302–315 (2015)
28. Q. Meng, X. Yan, Q. Ren, H. Adeli, Variable air volume air-conditioning experiment system with advanced controls. Indoor Built Environ. **25**(1), 114–127 (2014)
29. X. Pang, M.A. Piette, N. Zhou, Characterizing variations in variable air volume system controls. Energy Build. **135**, 166–175 (2017)
30. E.M. Saber, Performance evaluation of damper control settings for operation of multiple-zone variable air volume reheat system in different building applications and climate types. Build. Simul. **10**(5), 687–696 (2017)
31. K. Zhang, D.H. Blum, M. Grahovac, J. Hu, J. Granderson, M. Wetter. Development and verification of control sequences for single-zone variable air volume system based on ASHRAE guideline 36. Proceedings of the American Modelica Conference 2020, Boulder, Colorado, The United States of America. (2020)
32. K. Zhang, D. Blum, H. Cheng, G. Paliaga, M. Wetter, J. Granderson, Estimating ASHRAE guideline 36 energy savings for multi-zone variable air volume systems using spawn of EnergyPlus. J. Build. Perform. Simul. **15**(2), 215–236 (2022)
33. P. Kapalo, N. Spodyniuk, Effect of the variable air volume on energy consumption—case study. IOP

Conf. Series: Mater. Sci. Eng. **415**, 012027 (2018)

34. K. Alghamdi. Impact of implementing a dedicated outdoor air system in parallel with a multi-zone variable-air volume system on energy consumption, thermal comfort, and life cycle cost. Graduate Thesis, Dissertations, and Problem Reports, 3915. (2019)
35. S. Kaam, P. Raftery, H. Cheng, G. Paliaga, Time-averaged ventilation for optimized control of variable-air-volume systems. Energy Build. **139**, 465–475 (2017)
36. H.J. Kim, Y.H. Cho, A study on a control method with a ventilation requirement of a VAV system in multi-zone. Sustainability **9**(11), 2066 (2017)
37. K.H. Lee, K.I. Chin, J.H. Yoon, Effect of minimum airflow setting of VAV unit on building energy consumption under Korean climatic condition. Adv. Mater. Res. **450–451**, 1435–1439 (2012)
38. H.J. Ji, S.H. Yeon, J.W. Park, Y. Yoon, K.H. Lee, Machine Learning Based Simultaneous Control of Air Handling Unit Discharge Air and Condenser Water Temperatures Set-point for Minimized Cooling Energy in an Office Building, Energy Build. **297**, 113471 (2023)
39. D.B. Crawley, L.K. Lawrie, F.C. Winkelmann, W.F. Buhl, Y.J. Huang, C.O. Pedersen, R.K. Strand, R.J. Liesen, D.E. Fisher, M.J. Witte, J. Glazer, EnergyPlus: creating a new-generation building energy simulation program. Energy Build. **33**(4), 319–331 (2001)
40. S.H. Yeon, W.H. Kang, J.H. Lee, K.W. Song, Y.T Chae, K.H. Lee, Upper and Lower Threshold Limit of Chilled and Condenser Water Temperature Set-points During ANN Based Optimized Control, Energy Reports, **9**, 6349–6361 (2023)
41. The U.S. Department of Energy. Application guide for EMS. EnergyPlus Version 9.3.0 Documentation, Washington, The United States of America. (2020)
42. P.G. Ellis, P.A. Torcellini, D.B. Crawley. Simulation of energy management systems in EnergyPlus. Proceedings of Building Simulation, Beijing, China. (2007)
43. International Code Council (ICC). 2021 International energy conservation code (IECC). (2020)
44. P. Im, J.R. New, Y. Bae. Updated OpenStudio small and medium office prototype models. 16th IBPSA International Conference & Exhibition on Building Simulation 2019, Rome, Italy. (2019)
45. The U.S. Department of Energy. Input output reference. EnergyPlus Version 9.3.0 Documentation, Washington, The United States of America. (2020)
46. X. Lu, Z. Pang, Y. Fu, Z. O'Neill, Advances in research and applications of CO2-based demand-controlled ventilation in commercial buildings: a critical review of control strategies and performance evaluation. Build. Environ. **223**, 109455 (2022)
47. J. Park, J.H. Cha, Y. Yoon, K.H. Lee, Energy Characteristics of Multi-chiller Load Distribution Algorithms in a Large Office Building, Energy Build. **318**, 114462 (2024)
48. The U.S. Department of Energy. Engineering reference. EnergyPlus Version 9.3.0 Documentation, Washington, The United States of America. (2020)
49. American Society of Heating, Refrigerating and Air-Conditioning Engineers (ASHRAE). ASHRAE guideline 36, high-performance sequences of operation for HVAC systems. (2021)
50. J.H. Cha, J. Park, S.H. Yeon, Y. Yoon, K.H. Lee, Particle Swarm Optimization for Multichiller System: Capacity Configuration and Load Distribution. J. Build. Eng. **98**, 110953 (2024)
51. J.H. Cha, J.K. Park, C.H. Chi, S.H. Yeon, C.H. Kim, J.W. Moon, K.H. Lee, A New Integrated Framework to Fault Detection and Diagnosis of Air Handling Unit: Emphasizing the Impact of Symptoms. Energy Build. **319**, 114474 (2024)

## Authors and Affiliations


**Jong Man Lee[1] · Kwang Ho Lee[1] · Jin Woo Moon[2] · Sang Hoon Lee[3] · Tianzhen Hong[3]**

* Kwang Ho Lee
kwhlee@korea.ac.kr

[1] Department of Architecture, College of Engineering, Korea University, Seoul, Republic of Korea

[2] School of Architecture and Building Science, Chung-Ang University, Seoul, Republic of Korea

[3] Building Technology and Urban Systems Division, Lawrence Berkeley National Laboratory, Berkeley, USA